



OPEN

SUBJECT AREAS:
METALS AND ALLOYS
MECHANICAL PROPERTIESReceived
22 July 2013Accepted
3 February 2014Published
25 February 2014Correspondence and
requests for materials
should be addressed to
T.Z. (zhangtao@buaa.
edu.cn)

Microstructural percolation assisted breakthrough of trade-off between strength and ductility in CuZr-based metallic glass composites

Z. Q. Liu^{1,3}, G. Liu², R. T. Qu³, Z. F. Zhang³, S. J. Wu¹ & T. Zhang¹

¹Key Laboratory of Aerospace Materials and Performance (Ministry of Education), School of Materials Science and Engineering, Beihang University, Beijing 100191, P. R. China, ²State Key Laboratory for Mechanical Behavior of Materials, School of Materials Science and Engineering, Xi'an Jiaotong University, Xi'an 710049, P. R. China, ³Shenyang National Laboratory for Materials Science, Institute of Metal Research, Chinese Academy of Sciences, Shenyang 110016, P. R. China.

As two important mechanical properties, strength and ductility generally tend to be mutually exclusive in conventional engineering materials. The breakthrough of such a trade-off has been potentiated by the recently developed CuZr-based bulk metallic glass (BMG) composites ductilized by a shape memory CuZr(B2) phase. Here the microstructural dependences of tensile properties for the CuZr-based BMG composites were elucidated qualitatively and modeled quantitatively, and the underlying mechanisms were unraveled. Through the microstructural percolation induced by matching the length scales of particle size and interparticle spacing, a notable breakthrough was achieved in the composites that the general conflicts between strength and ductility can be defeated. This study is expected to greatly aid in the microstructural design and tailoring for improved properties of BMG composites. It also has implications for the development of strong and ductile materials in the future.

As two important mechanical properties, strength and ductility usually tend to be mutually exclusive in many classes of materials with the general rule that they are inversely related¹⁻³. The changes in a material's microstructural architecture often affect the strength and ductility in opposite ways, i.e. strengthening but sacrificing the ductility or alternatively ductilizing at a cost of strength. Thus a general trade-off between the two properties seems inevitable to make a compromise in developing strong and ductile materials. In particular, so far the structural applications of explored high-strength materials are usually limited by their relatively low ductility and toughness in engineering practice³. This is also the case for the emerging bulk metallic glasses (BMGs) which usually demonstrate extraordinarily high strength but disappointingly low ductility^{4,5}. The wide-spread structural applications of BMGs have been strictly limited by their macroscopic room-temperature brittleness and strain softening nature. It is revealed that these shortcomings can be mitigated by combining the glassy matrix with *in situ* formed ductile crystalline phases, i.e. forming BMG composites^{6,7}. In this respect, the CuZr-based BMG composites ductilized by a shape memory CuZr(B2) phase have attracted great attention in recent years owing to their outstanding mechanical properties⁸⁻¹². The unique transformation-mediated deformation mechanisms endow these composites with pronounced tensile ductility and work-hardening capacity without significantly sacrificing the high strength of the glassy matrix^{8,9}. In this scenario, the successful combination of shape memory alloys with BMGs may provide new opportunities to defeat the general conflicts between strength and ductility and open new avenues for the development of high-performance structural materials.

It is known that the mechanical properties of BMG composites depend strongly on their microstructures¹⁰⁻¹³. Thus the elucidation of the structure-property correlations is invariably essential for the microstructural design and tailoring to achieve intended mechanical properties. However, hitherto such an issue has rarely been discussed and still remains far from understood in terms of the tensile properties for the CuZr-based BMG composites¹¹. As a consequence, it still remains unclear and challenging about how to achieve the breakthrough of the trade-off relation between strength and ductility in the composites through controlling their microstructures. On the other hand, the percolation theory has been adopted to model the mechanical properties of several



BMG composites^{8,11,12,14}. It is supposed that the mechanical properties may be changed discontinuously when the microstructural percolation is achieved. Although such a percolation phenomenon has also been suggested in the CuZr-based BMG composites in previous studies^{8,11}, it still lacks systematic experimental results for verifying this hypothesis solidly and the critical percolation threshold has rarely been achieved so far. Moreover, it still remains mysterious about how the microstructure forms percolation as well as how and why the percolation affects the tensile properties of the composites. In this study, the tensile properties of a series of CuZr-based BMG composites with different microstructures have been examined and correlated to the microstructures systematically. The percolation is experimentally achieved by matching the characteristic microstructural length scales, giving solid evidence for this phenomenon in BMG composites. The underlying mechanisms for the percolation and the property variations are further unraveled. It is revealed that the integrated tensile properties of the present BMG composites indicate a notable breakthrough of the general trade-off between strength and ductility.

Results

The tensile properties and fractographic morphologies have been systematically evaluated and analyzed for the composites with different microstructures. Here we focus mainly on the structure-property relationships, and the readers are referred to the supplementary data for the detailed experimental results of representative samples. The dependences of the tensile yield strength σ_y and ultimate tensile strength σ_{UTS} on the crystalline volume fraction V_c in the composites are shown in Figure 1. It is seen that σ_y decreases monotonously with the increase in V_c throughout the entire crystallinity range. It has been revealed that the CuZr(B2) crystals precipitate from the alloys in a polymorphic manner that the compositions of the crystals and glassy matrix remain almost the same and identical to the nominal composition of the present alloy^{8,15}. As a result, the properties of the glassy matrix can be regarded to keep constant in the BMG composites with different V_c . On the other hand, the yielding of the CuZr(B2) phase is supposed to correspond to the initiation of its martensitic transformation^{12,16}. Such a process depends in principle on the electronic structure and stacking fault energy of the crystals which are closely related to the compositions^{16–18}. Thus it is reasonable to postulate that the yield strength of the CuZr(B2) phase also keeps constant in the composites as its composition remains unchanged. Therefore, based on the composite mechanics, a simple rule-of-mixtures can be adopted to elucidate the dependence of σ_y on V_c in the composites following

$$\sigma_y = \sigma_a V_a + \sigma_c V_c = \sigma_a(1 - V_c) + \sigma_c V_c, \quad (1)$$

where V and σ represent the volume fraction and yield strength of the constituents, and the subscripts a and c refer to the amorphous and crystalline phases, respectively. It is seen that the this approach is capable of describing the overall varying trend reasonably well (Figure 1(a)). Yet it is worth noting that there seems exist apparent asymmetry between the yield strengths under tension and compression for the composites⁸. It is reported that the rule-of-mixtures fails to capture the compressive yield strength when V_c exceeds $\sim 50\%$ wherein an alternative load-bearing model

$$\sigma_y = \sigma_c(1 + 0.5V_a) = \sigma_c(1.5 - 0.5V_c) \quad (2)$$

has been suggested⁸. However, this model is found to unreasonably underestimate the yield strength in tension, as indicated by the dashed pink line in Figure 1(a). In addition, careful examination further reveals that σ_y appears slightly higher than that predicted by the rule-of-mixtures in the vicinity of $\sim 50\%$ crystallinity as designated by the circled region. This is expected to be an indicative of the significant microstructural variations which will be discussed later.

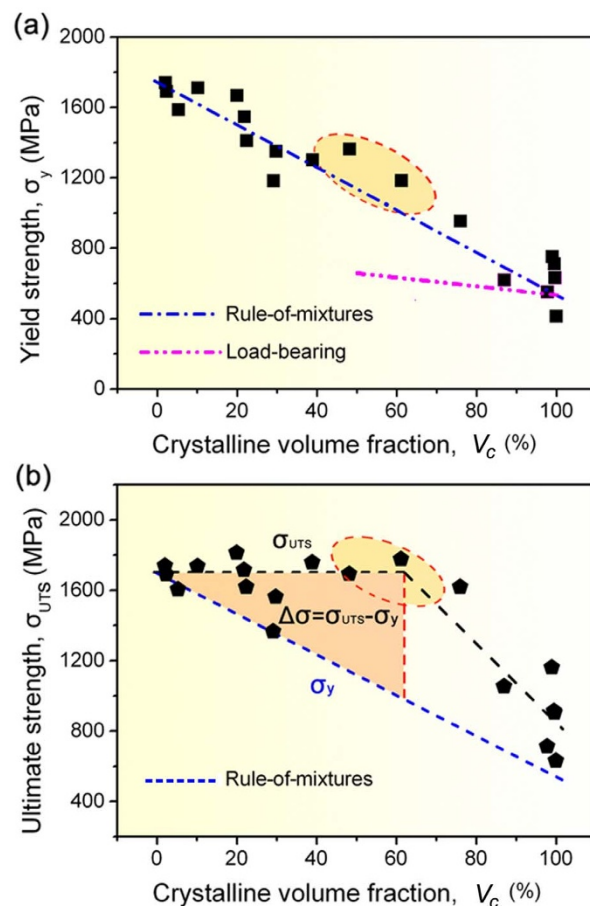


Figure 1 | Variations of tensile strength as a function of crystalline volume fraction. (a) The tensile yield strength σ_y can be roughly captured by the rule-of-mixtures. (b) The ultimate tensile strength σ_{UTS} remains almost constant for the composites with the crystalline volume fraction V_c lower than $\sim 60\%$ and then decreases steeply and linearly with the further increase in V_c .

In comparison, σ_{UST} remains almost constant around ~ 1700 MPa for the composites with V_c lower than $\sim 60\%$, which is analogous to the reported case for the compressive fracture strength¹⁰, and then decreases steeply and linearly with the further increase in V_c . The work-hardening capability can be preliminarily manifested by the stress window for the work-hardening process, i.e. the span between σ_{UTS} and σ_y , $\Delta\sigma = \sigma_{UTS} - \sigma_y$. It is seen that $\Delta\sigma$ increases almost linearly with the increase in V_c for the glass-dominated composites with V_c not exceeding $\sim 50\%$. This indicates an improved resistance of the composites to the macroscopic unstable flow localization.

Figure 2 shows the variation of the tensile ductility e_T as a function of V_c in the composites. It turns out that e_T exhibits a unimodal hump-shaped relation with V_c . It reaches its maximum value exceeding $\sim 10\%$ in the crystallinity range of $\sim 40\%$ – 70% and decreases steeply on both sides of the plateau. This can be described by adopting the percolation theory which is usually employed in understanding the discontinuous changes of physical properties in various random systems¹⁹. Recent studies have revealed that there exists a topological transition at a statistically critical microstructural condition in BMG composites where the microstructure is the most effective in hindering the propagation of shear bands^{8,11,14}. This transition can be termed as percolation and the transition point as the percolation threshold. Here by treating V_c as the key microstructural parameter, e_T can be modeled quantitatively by referring to the expressions of the percolation theory:

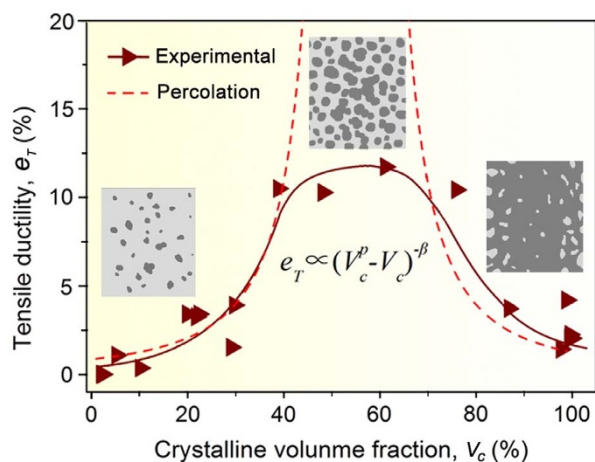


Figure 2 | Dependence of tensile ductility on crystalline volume fraction. The tensile ductility e_T can be quantitatively modeled using the percolation theory as denoted by the dashed curves. Representative microstructures of the composites with different crystalline volume fractions V_c are illustrated in the insets.

$$e_T \propto (V_c^p - V_c)^{-\beta}, \quad (3)$$

where V_c^p is the percolation threshold or the critical crystalline volume fraction to form microstructural percolation, and β is a power exponent¹⁹. The calculated results are proved to give a good description of the experimental data when the parameters V_c^p and β are quantified as 55% and 2 respectively in the composites. Moreover, it is noted that the whole crystallinity range has been covered systematically and the percolation threshold has been successfully achieved in the present study. These provide the solid evidence for the percolation phenomenon in the BMG composites.

Discussion

The variation in σ_{UST} can be correlated to the microstructural transition of the composites. The composites with low crystallinities can be regarded as the crystalline particle-ductilized BMG composites with CuZr(B2) crystals dispersed within the continuous glassy matrix. σ_{UST} is thus dominated by the shear fracture of the matrix which is essentially caused by the catastrophic propagation of shear bands²⁰. When V_c exceeds $\sim 50\%$, in comparison, the crystals begin to interconnect severely to form a crystalline skeleton in the composites and accordingly give rise to abundant grain boundaries. In this case, the overlapped crystals can be seen as the matrix and the glassy phase serves as the reinforcement. Then the global failure of the composites is controlled by the intergranular and transgranular fracture of the polycrystals^{10,11}. As a result, σ_{UST} depends not only on V_c but also on the grain size which is also crystallinity-related¹. Meanwhile, the increase in the density of grain boundaries is supposed to weaken the composites significantly. These account for the steep decrease in σ_{UST} with the further increase in V_c .

To uncover the origins of the percolation, the microstructural length scales of the crystalline particle size d and interparticle spacing λ have been measured for the composites with crystallinities lower than 50%, i.e. the glass-dominated composites. It is difficult to quantify their values for those with higher V_c due to the interconnection of individual particles. These length scales can be correlated to a characteristic material parameter of the glassy matrix—the plastic zone size ahead of a crack tip R_p , which can be expressed in terms of the yield strength and fracture toughness as

$$R_p = K_{IC}^2 / 2\pi\sigma_y^2, \quad (4)$$

where K_{IC} is the plane-strain fracture toughness^{4,6}. It is supposed that the shear bands tend to be stabilized against catastrophic

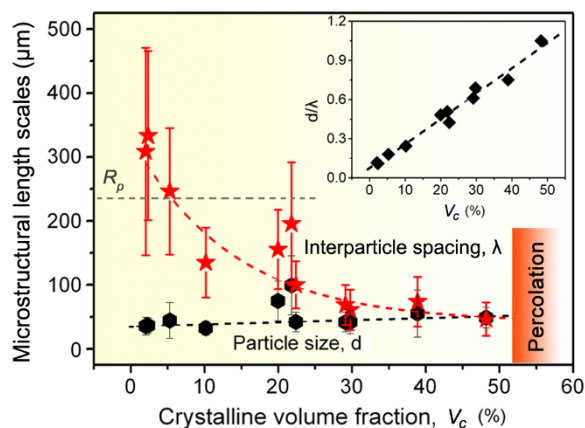


Figure 3 | Variations of microstructural length scales as a function of crystalline volume fraction. The crystalline particle size d increases gradually while the interparticle spacing λ decreases monotonously with the increase in the crystalline volume fraction V_c . Their ratio d/λ follows a positive linear relation with V_c , as shown in the inset.

propagation when their mean free path for propagation is smaller than this critical value. For the present system, R_p can be estimated to be $\sim 240 \mu\text{m}$ by adopting $K_{IC} \approx 70 \text{MPa}\sqrt{\text{m}^{21,22}}$.

As shown in Figure 3, λ decreases monotonously with the increase in V_c and falls below R_p when V_c exceeds $\sim 10\%$, while d increases gradually but locates beneath R_p all the way. In this manner, d and λ approach each other as V_c increases and their ratio d/λ follows a positive linear relation with V_c , as shown in the inset. In respect to their implications, d refers to the geometrical barrier for a shear band to penetrate through or detour around the particles, and λ represents the mean free path for the shear band acceleration or developing towards a crack, respectively. In the vicinity of $\sim 50\%$ crystallinity, the two length scales are nearly identical to each other (i.e. $d/\lambda \approx 1$) with a value of $\sim 50 \mu\text{m}$ which is smaller than the critical R_p . It is noted that the above crystallinity conforms well to the critical threshold for the microstructural percolation. In this scenario, the majority of the crystals are well dispersed within the continuous glassy phase in the composites, resulting in an ideally inter-dispersed structure with the two phases partitioned by each other, as shown in the insets in Figure 2. On the one hand, both the two microstructural length scales are smaller than but on the same scale with the critical R_p , giving rise to the predominance of stable shear banding rather than crack opening in the glassy matrix. On the other hand, the dimensions of the two phases match well with those of their ligaments. Thus the propagation of shear bands can be hindered effectively after a free path by the crystalline obstacles in the same scale. As a result, the microstructure plays the most effective role in improving the tensile properties of the composites.

The effects of the ratio d/λ on the mechanical properties can be further interpreted by simulating the stress distributions in the composites with different microstructures using the finite element modeling (FEM). Figure 4 illustrates the distributions of the equivalent von Mises stress in the composites with varying d/λ ratios at their corresponding global yield strains. It turns out that the crystalline phase tends to deform plastically prior to the amorphous matrix under an applied loading due to the large discrepancy between their yield strengths⁸. This causes distinct misfit in the local plastic strains between the two phases and thus creates significant stress concentrations adjacent to their interfaces^{23–25}. It is seen that the maximum stress is generated near the interfaces in the direction perpendicular to the loading axis and extends towards the neighboring particles, which is analogous to the reported case in the BMGs with designed pores²⁶. The direct results of such stress distributions can be mainly two-fold, i.e. to promote the initiation of shear bands at the interfaces

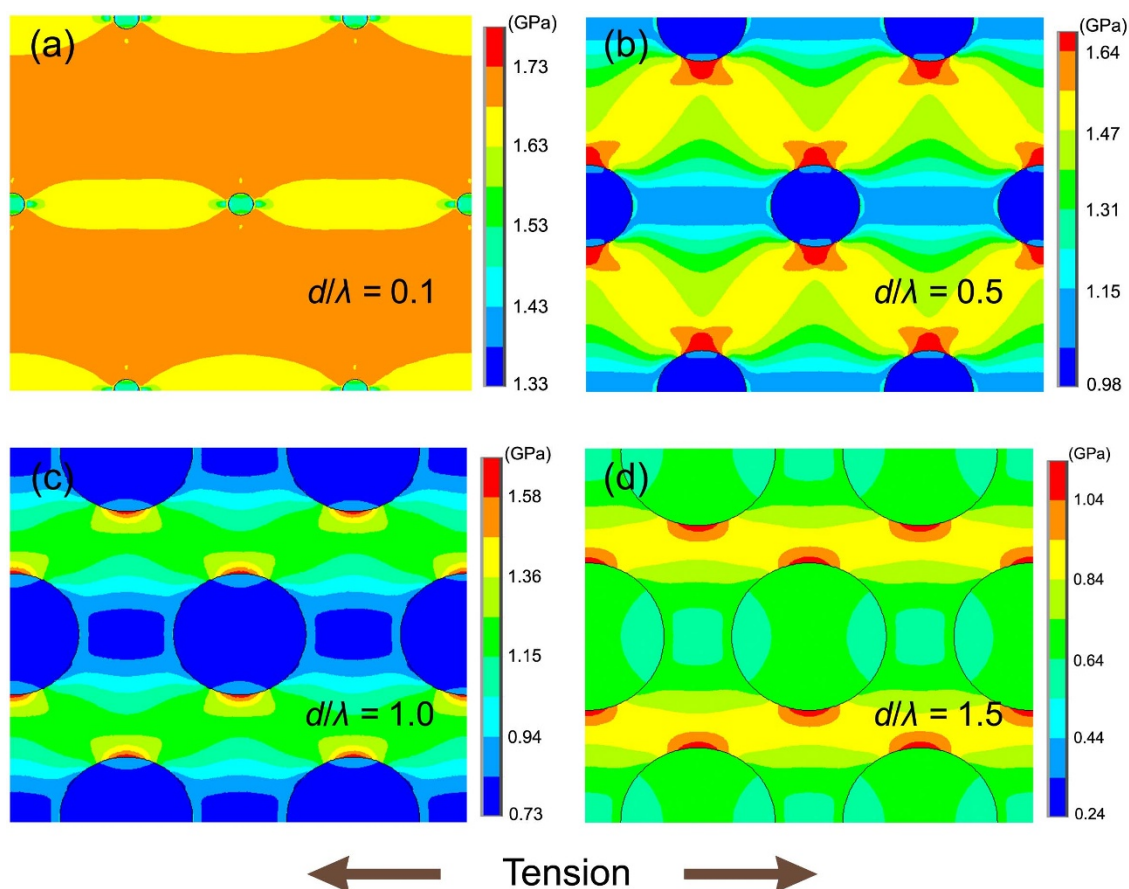


Figure 4 | Contour maps for the distributions of the equivalent von Mises stress in the composites with different microstructures. The corresponding global yield strains were applied for the composites with varying ratios between the crystalline particle size and interparticle spacing d/λ in the FEM simulation. The tensile loading direction was denoted by the arrows.

and to constrain them into the ligament regions between the neighboring particles. Meanwhile, the propagation of shear bands can be effectively hindered by the significant stress gradient, especially the steep stress drop, along the propagation path among the particles. The above effects on the shear bands render the composites with appreciable global tensile ductility in comparison with the monolithic BMGs. The cases for the distributions of the primary stress along the tensile axis have been further examined and are revealed to be almost the same or even more evident (see the supplementary data).

The simultaneous increase in d/λ and V_c tends to enlarge the local strain misfit between the crystalline phase and amorphous matrix, and accordingly results in intensified stress concentrations near their interfaces. This facilitates the initiation of shear bands to a higher degree and makes it possible at even lower global stresses. At the same time, the propagation of shear bands can be hindered more effectively owing to the lowered global stress level and the increased stress gradient along their paths. As a consequence, the tensile ductility of the composites can be improved markedly as manifested by the left side of the plateau in Figure 2. Moreover, it is seen that such microstructural variation tends to decrease the angle between the preferred shear band plane and the global loading axis. Besides, the concordance between the stress concentrations on the upper and lower sides of each particle is gradually degraded along the inclined shear direction. These are also expected to retard the unstable propagation of shear bands and prevent their premature coalescence by tuning their propagation path to deviate from the favored one²⁷, and thus contribute to better ductility. With the further increase in d/λ to exceed ~ 1 , however, the stress concentrations around neighboring particles begin to overlap severely in the ligament regions. This

results in a high stress level and decreases the stress gradient in the amorphous matrix and hence deteriorates the hindering effect on the propagation of shear bands. Such a case can also be manifested by the stress distribution in the composites near the global fracture strain which is shown in the supplementary data. Also, the ligament regions become too thin that can be easily penetrated by the shear bands. As a result, the global ductility is supposed to be deteriorated seriously in accordance with the right part of the plateau in Figure 2. Furthermore, in a practical view, it is difficult to avoid the impingement of the crystalline particles experimentally in the rapid solidification process when V_c is high. Thus weak grain boundaries may be introduced into the composites, which are also detrimental to the global ductility¹¹.

According to the above results and discussion, the CuZr-based BMG composites demonstrate tunable combinations of tensile properties strongly depending on their microstructures. As the strength and ductility are usually major focuses in tension, a map integrating the two properties can be constructed for the composites. As shown in Figure 5(a), the composites display variable ductility e_T while still maintaining very high strengths of σ_y and σ_{UST} owing to the synergistic effects of the constituents. Their strength-ductility relationships deviate evidently from the conventional inversely proportional relations in engineering alloys as qualitatively denoted by the dashed curve¹⁻³. Thus a notable exception is achieved that the mechanical properties can be intentionally tailored to defeat the general conflicts between strength and ductility and thus break through the trade-off between them. The pronounced combinations of high strength and good ductility can be readily obtained through the microstructural percolation by matching the length scales of crystalline particle size and interparticle spacing in the BMG composites. This is expected to

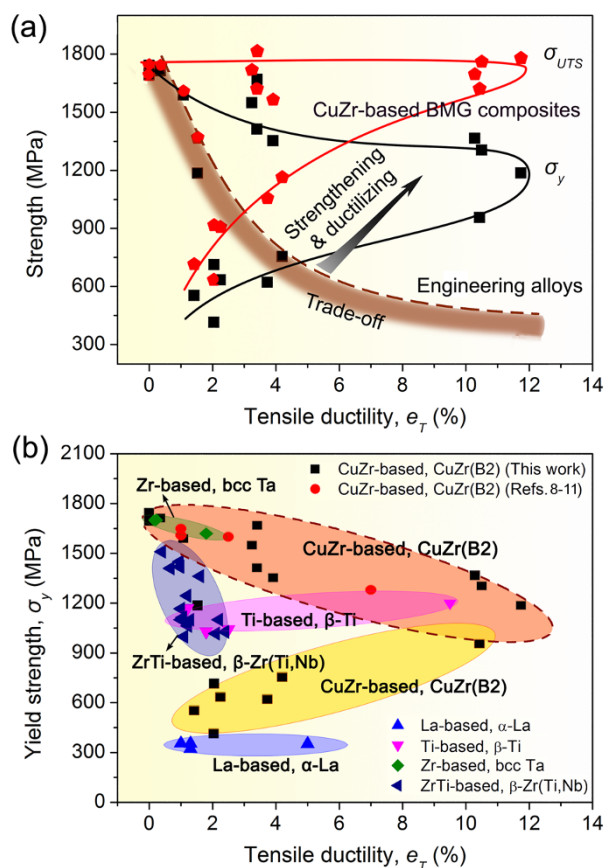


Figure 5 | Integrated tensile properties of strength and ductility for BMG composites. (a) The strength-ductility relationships of the present CuZr-based BMG composites deviate evidently from the conventional inversely proportional relation in engineering alloys as qualitatively denoted by the dashed curve. (b) The present composites are superior in tensile properties among various BMG composites in different systems ductilized by different crystalline phases^{6,8–11,22,24,28–33}.

provide novel strategies for defeating the general strength-ductility conflicts and achieving both high strength and good ductility in materials. Furthermore, to give an intuitive evaluation of the mechanical properties, the tensile properties of other BMG composites are further collected from literatures and illustrated in Figure 5(b) regardless of their variant gauge dimensions^{6,8–11,22,24,28–33}. It is seen explicitly that the present composites extend a wide range of superior σ_y - e_T combinations among various BMG composites. In particular, the combinations of variable e_T with high σ_y , as designated by the dashed circle, serve as the potential candidates for tailoring the mechanical properties of the composites. This usually requires the fine-tuning of microstructures through adopting different compositions or processing routes such as melt adjustment and laser surface melting^{6,11,34,35}. It is anticipated that the present composites demonstrate great potentials for structural applications owing to their superior and tunable mechanical properties and may find their practical use in the near future.

In summary, the tensile strength and ductility of CuZr-based BMG composites show strong dependences on the microstructures and their microstructural dependences were described using different approaches. The composites exhibit notable integrated tensile properties through the microstructural percolation induced by matching the characteristic microstructural length scales of crystalline particle size and interparticle spacing. The percolation theory has been adopted in several BMG composites, including the CuZr-based ones, to model their mechanical properties^{8,11,12,14}, yet the

underlying physics still remain mysterious. Here the whole crystallinity range was covered systematically, providing the direct and solid evidences for the percolation phenomenon in BMG composites. Furthermore, the mechanisms of the microstructural percolation and the variations in the mechanical properties were unraveled in terms of the initiation and propagation of shear bands. The combinations of tensile strength and ductility of the present BMG composites may help defeat the general conflicts between strength and ductility and break through the trade-off between them. This study might give deep insights on the critical issue of the structure-property correlations in the BMG composites and greatly aid in their microstructural design and tailoring to achieve intended mechanical properties. It may further provide new strategies for defeating the general strength-ductility conflicts in materials and for developing strong and ductile materials in the future.

Methods

Alloy ingots in the composition of $\text{Cu}_{47.5}\text{Zr}_{47.5}\text{Al}_5$ (at.%) were obtained by arc-melting the mixtures of pure constituent elements under Ti-gettered high-purity argon atmosphere. Cylindrical rods with a diameter of 3 mm and a length of ~ 45 mm were prepared by copper mold casting. To obtain various microstructures, the casting temperatures were varied manually by applying different melting currents for randomly different melting time³⁶. Twenty dog-bone shaped specimens for tensile tests with a gauge diameter of 1.5 mm and a gauge length of 6 mm were machined and polished from different sections along the length of the as-cast rods. Tensile tests were conducted at a strain rate of $3 \times 10^{-4} \text{ s}^{-1}$ at room temperature in air. Here the tensile ductility e_T was defined as the true tensile plastic strain between the yield strain and the total strain at the ultimate tensile strength σ_{UTS} . Morphologies of the fractured samples were analyzed using a CamScan 3400 scanning electron microscope (SEM). The microstructures of the specimens were characterized by examining the transverse sections adjacent to the same ends of the slender regions by an electron probe microanalyzer using the backscattered electron (BSE) mode. The volume fractions of the crystalline phase in the composites were estimated from its area proportions in the BSE images^{8–13}. Based on the quantitative microscopy³⁷, the interparticle spacing (λ) was measured by superposing random lines on the BSE micrographs of the composites and the values were determined from the number of particles intercepting the testing line, N , and the total length between the two outermost particles (L) as $\lambda = L/(N - 1)$ ³⁸. Forty random lines intercepting at least two particles were superposed on the micrographs for each sample. Finite element modeling (FEM) was conducted to simulate the stress and strain distributions in the composites with different microstructures. An AB-type stacking for the crystalline particles was considered to model the microstructures²⁶. The amorphous matrix was treated as elastic-perfectly plastic with no work-hardening capability²³, and a stable work-hardening behavior was assumed for the crystalline phase. The properties of the two constituent phases were collected from literatures⁸ and also listed in the supplementary data.

1. Ashby, M. F. *Materials Selection in Mechanical Design* (Butterworth-Heinemann, Oxford, 2011).
2. Ritchie, R. O. The conflicts between strength and toughness. *Nature Mater.* **10**, 817–822 (2011).
3. Launey, M. E. & Ritchie, R. O. On the fracture toughness of advanced materials. *Adv. Mater.* **21**, 2103–2110 (2009).
4. Ashby, M. F. & Greer, A. L. Metallic glasses as structural materials. *Scripta Mater.* **54**, 321–326 (2006).
5. Liu, Z. Q. *et al.* Quasi phase transition model of shear bands in metallic glasses. *Acta Mater.* **59**, 7416–7424 (2011).
6. Hofmann, D. C. *et al.* Designing metallic glass matrix composites with high toughness and tensile ductility. *Nature* **451**, 1085–1089 (2008).
7. Cheng, J. L., Chen, G., Liu, C. T. & Li, Y. Innovative approach to the design of low-cost Zr-based BMG composites with good glass formation. *Sci. Rep.* **3**, 2097; doi:10.1038/srep02097 (2013).
8. Pauly, S. *et al.* Microstructural heterogeneities governing the deformation of $\text{Cu}_{47.5}\text{Zr}_{47.5}\text{Al}_5$ bulk metallic glass composites. *Acta Mater.* **57**, 5445–5453 (2009).
9. Wu, Y., Xiao, Y. H., Chen, G. L., Liu, C. T. & Lu, Z. P. Bulk metallic glass composites with transformation-mediated work-hardening and ductility. *Adv. Mater.* **22**, 2770–2773 (2010).
10. Wu, Y. *et al.* Relationship between composite structures and compressive properties in CuZr-based bulk metallic glass system. *Chin. Sci. Bull.* **56**, 3960–3964 (2011).
11. Liu, Z. Q. *et al.* Microstructural tailoring and improvement of mechanical properties in CuZr-based bulk metallic glass composites. *Acta Mater.* **60**, 3128–3139 (2012).
12. Song, K. K. *et al.* Correlation between the microstructures and the deformation mechanisms of CuZr-based bulk metallic glass composites. *AIP Adv.* **3**, 012116 (2013).



13. Narayan, R. L. *et al.* On the microstructure-tensile property correlations in bulk metallic glass matrix composites with crystalline dendrites. *Acta Mater.* **60**, 5089–5100 (2012).
14. Fu, X. L., Li, Y. & Schuh, C. A. Mechanical properties of metallic glass matrix composites: Effects of reinforcement character and connectivity. *Scripta Mater.* **56**, 617–620 (2007).
15. Pauly, S., Das, J., Duhamel, C. & Eckert, J. Martensite formation in a ductile Cu_{47.5}Zr_{47.5}Al₅ bulk metallic glass composite. *Adv. Eng. Mater.* **9**, 487–491 (2007).
16. Song, K. K. *et al.* Triple yielding and deformation mechanisms in metastable Cu_{47.5}Zr_{47.5}Al₅ composites. *Acta Mater.* **60**, 6000–6012 (2012).
17. Wu, Y. *et al.* Ductilizing bulk metallic glass composites by tailoring stacking fault energy. *Phys. Rev. Lett.* **109**, 245506 (2012).
18. Zhou, D. Q. *et al.* Alloying effects on mechanical properties of the Cu-Zr-Al bulk metallic glass composites. *Comput. Mater. Sci.* **79**, 187–192 (2013).
19. Nan, C. W. Physics of inhomogeneous inorganic materials. *Prog. Mater. Sci.* **37**, 1–116 (1993).
20. Zhang, Z. F., Eckert, J. & Schultz, L. Difference in compressive and tensile fracture mechanisms of Zr₅₉Cu₂₀Al₁₀Ni₈Ti₃ bulk metallic glass. *Acta Mater.* **51**, 1167–1179 (2003).
21. Kumar, G., Desai, A. & Schroers, J. Bulk metallic glass: The smaller the better. *Adv. Mater.* **23**, 461–476 (2011).
22. Liu, Z. Q. *et al.* Pronounced ductility in CuZrAl ternary bulk metallic glass composites with optimized microstructure through melt adjustment. *AIP Adv.* **2**, 032176 (2012).
23. Ott, R. T. *et al.* Micromechanics of deformation of metallic-glass-matrix composites from in situ synchrotron strain measurements and finite element modeling. *Acta Mater.* **53**, 1883–1893 (2005).
24. Zhu, Z., Zhang, H., Hu, Z., Zhang, W. & Inoue, A. Ta-particulate reinforced Zr-based bulk metallic glass matrix composite with tensile plasticity. *Scripta Mater.* **62**, 278–281 (2010).
25. Qiao, J. W. *et al.* A tensile deformation model for in-situ dendrite/metallic glass matrix composites. *Sci. Rep.* **3**, 2816 (2013).
26. Sarac, B. & Schroers, J. Designing tensile ductility in metallic glasses. *Nature Commun.* **4**, 2158 (2013).
27. Qu, R. T., Zhao, J. X., Stoica, M., Eckert, J. & Zhang, Z. F. Macroscopic tensile plasticity of bulk metallic glass through designed artificial defects. *Mater. Sci. Eng. A* **534**, 365–373 (2013).
28. Qiao, J. W. *et al.* Tensile deformation micromechanisms for bulk metallic glass matrix composites: From work-hardening to softening. *Acta Mater.* **59**, 4126–4137 (2011).
29. Kim, C. P., Oh, Y. S., Lee, S. & Kim, N. J. Realization of high tensile ductility in a bulk metallic glass composite by the utilization of deformation-induced martensitic transformation. *Scripta Mater.* **65**, 304–307 (2011).
30. Lee, M. L., Li, Y. & Schuh, C. A. Effect of a controlled volume fraction of dendritic phases on tensile and compressive ductility in La-based metallic glass matrix composites. *Acta Mater.* **52**, 4121–4131 (2004).
31. Oh, Y. S., Kim, C. P., Lee, S. & Kim, N. J. Microstructure and tensile properties of high-strength high-ductility Ti-based amorphous matrix composites containing ductile dendrites. *Acta Mater.* **59**, 7277–7286 (2011).
32. Szuëcs, F., Kim, C. P. & Johnson, W. L. Mechanical properties of Zr_{56.2}Ti_{13.8}Nb_{5.0}Cu_{6.9}Ni_{5.6}Be_{12.5} ductile phase reinforced bulk metallic glass composite. *Acta Mater.* **49**, 1507–1513 (2001).
33. Fan, C., Ott, R. T. & Hufnagel, T. C. Metallic glass matrix composite with precipitated ductile reinforcement. *Appl. Phys. Lett.* **81**, 1020–1022 (2002).
34. Qiao, J. W., Wang, S., Zhang, Y., Liaw, P. K. & Chen, G. L. Large plasticity and tensile necking of Zr-based bulk-metallic-glass-matrix composites synthesized by the Bridgman solidification. *Appl. Phys. Lett.* **94**, 151905 (2009).
35. Wu, G. J. *et al.* Induced multiple heterogeneities and related plastic improvement by laser surface treatment in CuZr-based bulk metallic glass. *Intermetallics* **24**, 50–55 (2012).
36. Mao, J. *et al.* The effects of casting temperature on the glass formation of Zr-based metallic glasses. *Adv. Eng. Mater.* **11**, 986–991 (2009).
37. DeHoff, R. T. & Rhines, F. N. *Quantitative Microscopy* (McGraw-Hill, New York, 1968).
38. Underwood, E. E. *Metals Handbook* (ASM International, Metals Park, OH, 1985).

Acknowledgments

This work was supported by the National Natural Science Foundation of China (Grant Nos. 51131002 and 51331007) and the IMR SYNL-T.S. Kê Research Fellowship.

Author contributions

Z.Q.L. and T.Z. proposed the idea and designed the research plan. Z.Q.L. and G.L. carried out the experiments and collected the data. R.T.Q. conducted the simulation. Z.Q.L., G.L., R.T.Q., Z.F.Z. and S.J.W. analyzed the data and wrote the paper. T.Z. revised the paper and approved it.

Additional information

Supplementary information accompanies this paper at <http://www.nature.com/scientificreports>

Competing financial interests: The authors declare no competing financial interests.

How to cite this article: Liu, Z.Q. *et al.* Microstructural percolation assisted breakthrough of trade-off between strength and ductility in CuZr-based metallic glass composites. *Sci. Rep.* **4**, 4167; DOI:10.1038/srep04167 (2014).



This work is licensed under a Creative Commons Attribution-NonCommercial-ShareAlike 3.0 Unported license. To view a copy of this license, visit <http://creativecommons.org/licenses/by-nc-sa/3.0>